Elastic-plastic behaviour of thin tubes subjected to internal pressure and intermittent high-heat fluxes with application to fast-nuclear-reactor fuel elements

J Bree

The Journal of Strain Analysis for Engineering Design 1967 2: 226
DOI: 10.1243/03093247V023226

ELASTIC–PLASTIC BEHAVIOUR OF THIN TUBES SUBJECTED TO INTERNAL PRESSURE AND INTERMITTENT HIGH-HEAT FLUXES WITH APPLICATION TO FAST-NUCLEAR-REACTOR FUEL ELEMENTS

J. BREE *Mathematics Department, Heriot-Watt University, Edinburgh; formerly Dounreay Experimental Reactor Establishment*

A sealed reactor fuel can when subjected to sufficiently high thermal stresses in the presence of an internal pressure will yield plastically. A simple model of the can is used to show that the plastic strains so produced may cause ratchetting or plastic cycling as the temperature gradient across the can wall cycles because of start-up and shutdown of the reactor. On the assumption that creep is negligible, approximate criteria are derived for the onset of ratchetting and plastic cycling, simple expressions are obtained for the plastic strains incurred by each cycle, and failure of the can due to the above mechanisms is discussed both for work-hardening and non-work-hardening material. Consideration is then given to the effect of stress relaxation due to creep when the mean temperature of the can is sufficiently high to cause complete relaxation of the thermal stress while the reactor is at power, creep being ignored while the reactor is shut down. Under these conditions, it is found that the criterion for ratchetting is simply the criterion for plastic yielding during the first temperature cycle. Finally, it is shown in an appendix that the results obtained from the simple model also hold, with minor modifications, for the similar problem of a thin spherical shell subjected to an internal pressure and a temperature gradient across the shell wall which is cycled. Use is made of this to discuss the accuracy of the results obtained from the simple model when applied to a thin can.

INTRODUCTION

A PROBLEM of current interest in the design of fast-nuclear-reactor fuel elements is the determination of the strain behaviour of the cladding material, or the fuel can, under the combined effects of internal gas pressure and intermittent high-heat fluxes. The can wall is subjected to a large temperature gradient while the reactor is at power and zero temperature gradient while the reactor is shut down. Consequently, the can experiences high thermal stresses which vary cyclically with start-up and shutdown of the reactor. The internal pressure is due to the release of gaseous fission products from the fuel which is contained within the can. The pressure therefore increases with burn-up and hence with time. However, in the present paper we are concerned primarily with the physical phenomena which result from interaction of the cyclic stresses with the pressure stress. It is therefore assumed in the subsequent analysis that the pressure stress is constant. If the combined thermal and pressure stress, calculated on a purely elastic basis, exceeds the yield limit in any region, the can material will flow plastically to maintain the stress in that region at its limiting value (the yield stress). Since the plastic strains so produced are non-uniform and irreversible with stress in the thermodynamic sense, residual stresses are produced in the can material when the reactor is shut down and these in turn may be sufficiently large to cause further plastic flow. In this manner plastic strains may be incurred by each start-up and shutdown of the reactor. Behaviour of this type gives rise to two possible modes of can failure and so constitutes one of the limiting factors in the design of an unvented fuel element.

Under certain stress conditions, unidirectional plastic strains are produced during each temperature cycle and these, owing to their irreversible nature, have a cumulative effect which causes progressive growth of the can or ratchetting. Since ratchetting has an adverse effect on coolant flow rate and can ultimately lead to rupture, it is necessary to have some knowledge of the loading conditions which enable ratchetting to occur and to be able to estimate the increment of strain per cycle. Plastic cycling presents another possible mode of can failure. Here plastic flow occurs during each temperature cycle, but where the plastic strain is tensile during one part of the cycle, it has the same magnitude but is compressive during the other part of the cycle so that these cancel, there being no net growth of the can. Nevertheless, this form of repeated straining in the plastic range ultimately causes fatigue cracking. It is therefore desirable to know when plastic cycling occurs and to be able to estimate the range of variation of the plastic strain which, according to Coffin's fatigue law (1)*, determines the number of cycles to failure. The problem presented above is further complicated by the effect of creep when it occurs.

Since a number of different effects have to be accounted for, it is convenient to divide the paper into separate sections. In the first section, a simple uniaxial-stress model of the can is developed and the equations which determine

The MS. of this paper was first received at the Institution of Mechanical Engineers on 11th July 1966 and in its revised form, as accepted by the Council for publication, on 22nd February 1967. 23

* *References are given in Appendix 4.*

the solution of the problem are presented. The problem is then investigated in the second section for non-work-hardening material with a yield stress independent of temperature, the criteria for the onset of ratchetting and plastic cycling first obtained by Miller (2) are derived, and estimates are made of the plastic strains incurred by each cycle. In the third section, similar criteria and the plastic strains produced per cycle are derived for a material whose yield stress on start-up differs from its value on shutdown owing to changes in mean temperature. Some consideration is then given in the fourth section to the effect of work-hardening on the Miller criteria and on the plastic strains produced per cycle. Finally, in the fifth section, an attempt is made to include the worst possible effect of creep by assuming that the stress is relaxed by creep to its limiting value while the reactor is at power, creep being ignored while the reactor is shut down. In addition, it is assumed that the can material has a uniform creep strength. However, the effect of non-uniform creep strength due to non-uniform temperature is discussed in Appendix 3.

It is shown in Appendix 1 that the results obtained by means of the uniaxial-stress model also apply, with minor modification, to the similar problem of a thin spherical shell subjected to an internal pressure and a cyclic temperature gradient across its wall. The more accurate biaxial model of the can is then considered to some extent in Appendix 2. Use is made of the results of Appendices 1 and 2 to discuss the theoretical accuracy of the results obtained from the uniaxial model when applied to a thin can.

Notation

a, b, c, a_n, b_n	x co-ordinates of elastic–plastic boundaries.
d	Can-wall thickness.
E	Young's modulus.
E_1	Slope of plastic part of the uniaxial stress–strain curve.
k	Defined by equation (30) (approximately equal to E_1 when $E_1 \ll E$).
N	Number of cycles to failure under plastic cycling.
n	Number of cycles experienced by the can.
P	Pressure.
R	Can mean radius.
T	Temperature.
ΔT	Temperature drop across the can wall.
x	Co-ordinate measured radially outwards from the can mid-wall.
α	Thermal coefficient of linear expansion.
δ	Ratchet strain per cycle.
ϵ	Total strain.
ϵ_c	Maximum value of plastic strain range.
$\epsilon_c^{(n)}$	Increase in total strain due to creep while the reactor is at power during the nth cycle.
ϵ_f	Tensile ductility.
η	Total plastic or creep strain.
η_n	Plastic strain incurred by the nth start-up.
η'_n	Plastic strain incurred by the nth shutdown.
$\eta_c^{(n)}$	Creep strain incurred by the nth cycle.
λ	Ratio of σ_L to σ_p.
λ_1	Value of λ at inner surface of the can.
ν	Poisson's ratio.
σ	Stress.
σ_L	Limiting stress distribution after stress relaxation due to creep while the reactor is at power.
σ_p	Pressure stress.
σ_t	Maximum value of elastic thermal stress.
σ_y	Yield stress when reactor is at power.
σ'_y	Yield stress when reactor is shut down if different from σ_y.

THE UNIAXIAL STRESS MODEL

Development of the model

To develop the simple model on which the subsequent analysis is based, first consider the can to be represented by a hollow cylinder of mean radius R and wall thickness d which is closed at both ends. Let the can be subjected to an internal pressure p, zero external pressure, and a cylindrically symmetrical heat flux through its inner surface which causes the temperature drop across the can wall to be cycled between ΔT and zero.

It is assumed that the length of the can is very much greater than its width and that d is very much less than R so that end effects and the effects of curvature may be neglected. The hoop and axial strains, ϵ_θ and ϵ_z, are then the same for each element at each stage of the deformation while the hoop and axial stresses, σ_θ and σ_z, depend only on the co-ordinate x measured radially outwards from the can mid-wall. For equilibrium in the radial and axial directions, we require

$$\int_{-1/2d}^{1/2d} \sigma_\theta \, dx = 2\int_{-1/2d}^{1/2d} \sigma_z \, dx = PR/d \quad . \quad (1)$$

that is, for a long thin can σ_θ and σ_z have mean values σ_p and $\frac{1}{2}\sigma_p$, respectively, where

$$\sigma_p = PR/d \quad . \quad . \quad . \quad . \quad (2)$$

In comparison with this the radial stress may be neglected. Further, when measured relative to the can mid-wall, the temperature distribution is given approximately by

$$T = -\Delta Tx/d \quad . \quad . \quad . \quad . \quad (3)$$

during the first half of each cycle (start-up) and is zero during the second half of each cycle (shutdown). The thin can may therefore be regarded as a two-dimensional slab (Fig. 1), subjected to mean stresses σ_p and $\frac{1}{2}\sigma_p$ in the hoop and axial directions, respectively, and prevented from bending in both these directions upon application and removal of the above temperature distribution.

The elastic solutions for the stresses in a thin can are (3) (4)

$$\sigma_\theta = \sigma_p + 2x\sigma_t/d, \quad \sigma_z = \sigma_p/2 + 2x\sigma_t/d \quad . \quad (4)$$

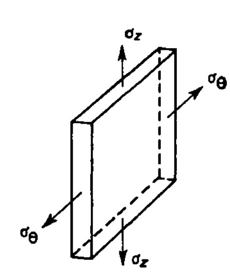

Fig. 1. Biaxial stress model of thin can

where

$$\sigma_t = E\alpha\Delta T/2(1-\nu) \quad . \quad . \quad . \quad (5)$$

is the maximum value of the elastic thermal stress which varies between $-\sigma_t$ at $x = -\frac{1}{2}d$ and σ_t at $x = \frac{1}{2}d$. Even for this relatively simple biaxial model of the can, the solution for the stresses and strains when the material yields plastically can only be obtained numerically (see Appendix 2). However, the model may be simplified further if we consider the stress in the hoop direction only, which is the dominant stress, and assume that the axial stress is zero. Physically this may be achieved by letting the mean stress in the axial direction be zero and allowing the slab to bend freely in that direction as shown in Fig. 2*a*, so that the thermal stress in the axial direction is also zero. Thus the slab is subjected to a mean stress σ_p in one direction only, corresponding to the hoop direction, and prevented from bending in that direction on both application and removal of the temperature gradient. Fig. 2*b* illustrates the cross-section of the uniaxial model in the direction of the applied stress. Under these conditions the combined pressure and thermal elastic hoop stress is given by

$$\sigma = \sigma_p + E\alpha\,\Delta T'x/d \quad . \quad . \quad . \quad (6)$$

where the suffix θ has been dropped since the problem is now uniaxial in stress and $\Delta T'$ denotes the temperature difference for the uniaxial model. On comparing this with the first of equations (4) we find that the factor $(1-\nu)^{-1}$ is no longer present in the thermal stress. However, it is believed that the stress in the uniaxial model can be made to simulate the hoop stress in the can with reasonable accuracy by taking

$$\Delta T' = \Delta T/(1-\nu) \quad . \quad . \quad . \quad (7)$$

On substituting for $\Delta T'$ in equation (6), σ may be written in the form

$$\sigma = \sigma_p + 2x\sigma_t/d \quad . \quad . \quad . \quad . \quad (8)$$

which, for purely elastic deformations, equals the hoop stress in a thin can.

Even with this artifice, it should be emphasized that we are not completely justified in neglecting the axial stress. Nevertheless, the model so obtained still contains the essential physical features of the problem and yields simple analytic solutions. Consequently it provides a better qualitative understanding of the problem than could be gained from a detailed numerical solution. Clearly, under the hoop stress alone the can grows radially, whereas under the axial stress alone it contracts radially so that the effect of the axial stress is to oppose the hoop stress and hence, in this sense, the results predicted by the simple model will be pessimistic. Although the precise numerical significance of neglecting the axial stress is not immediately clear, certain general conclusions can be made in this respect and these are discussed later.

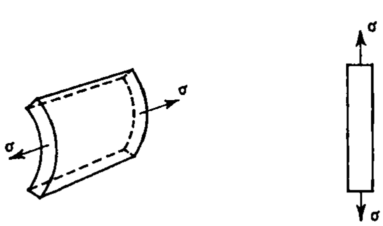

a Three-dimensional view.
b Cross-section in direction of applied stress.

Fig. 2. Uniaxial stress model of thin can

Statement of the simplified problem

The problem is now reduced to finding the deformation in a slab when subjected to a uniaxial stress σ of mean value σ_p which acts against differential thermal expansion and contraction to prevent bending in its own direction on both application and removal of the temperature distribution

$$T = -\Delta T'x/d \quad . \quad . \quad . \quad . \quad (9)$$

If the total strain in the direction of the applied stress is denoted by ϵ, the condition that bending is prevented is expressed by the equation

$$\epsilon = \text{constant} \quad . \quad . \quad . \quad . \quad (10)$$

although this constant may vary from one half cycle to the next, and the mean stress condition may be written

$$\int_{-1/2d}^{1/2d} \sigma \, dx = \sigma_p d \quad . \quad . \quad . \quad (11)$$

For a uniaxially applied stress in non-work-hardening material both the von Mises and Tresca yield criteria (5) reduce to

$$\left.\begin{array}{ll} |\sigma| = \sigma_y & \text{(in plastic regions)} \\ |\sigma| < \sigma_y & \text{(in elastic regions)} \end{array}\right\} \quad . \quad (12)$$

where σ_y is the yield stress. Thus $|\sigma|$ cannot exceed σ_y, and in regions where the stress tends to exceed the yield stress elastically plastic strains are introduced to maintain the stress at its limiting value. The yield criterion for work-hardening material with a linear rate of hardening is discussed in the fourth section.

Finally, the uniaxial stress–strain relation may be written

$$\epsilon = \sigma/E + \alpha T + \eta \quad . \quad . \quad . \quad (13)$$

where σ/E is the elastic strain, αT is the thermal strain, and η is the plastic strain. On substituting for T, the stress–strain relation for the first half of each cycle is found to have the form

$$E\epsilon = \sigma - 2x\sigma_t/d + E\eta \quad . \quad . \quad . \quad (14)$$

For the second half of each cycle the temperature gradient is removed so that the stress–strain relation becomes

$$E\epsilon = \sigma + E\eta \quad . \quad . \quad . \quad . \quad (15)$$

We therefore require to solve equations (14) and (15) for the stresses and strains during each cycle subject to the conditions (10), (11), and (12).

Certain general properties of the solution are already apparent from the above equations. For the first half of each cycle equation (14) holds and since ϵ is independent of x, $\sigma + E\eta$ is linear in x with slope $2\sigma_t/d$. For example, in regions of the can where $E\eta$ is uniform, σ has slope $2\sigma_t/d$ and vice versa. For the second half of each cycle equation (15) holds and since ϵ is uniform, $\sigma + E\eta$ is uniform across the can wall. Thus, for the second half of each cycle, σ and $E\eta$ have equal and opposite slopes at each point in the can.

NON-WORK-HARDENING MATERIAL WITH YIELD STRESS INDEPENDENT OF TEMPERATURE

Here the strain behaviour of the can material depends on the stress régimes shown in Fig. 3. Ratchetting occurs if

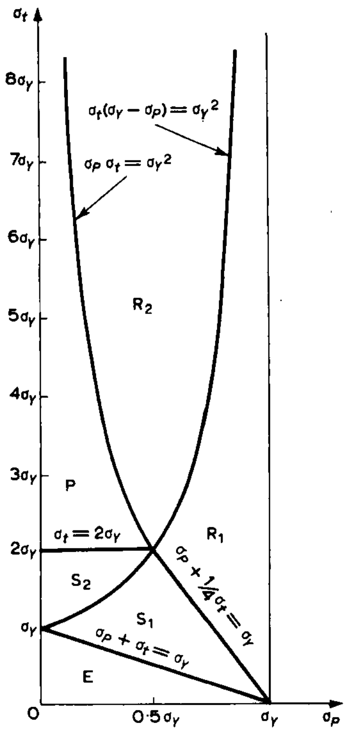

Stress régime	Can behaviour
R_1 and R_2	Ratchetting
S_1 and S_2	Shakedown after first half-cycle
P	Plastic cycling
E	Elastic

Fig. 3. Stress régimes for non-work-hardening material whose yield stress σ_Y remains unchanged by changes in mean temperature

(σ_p, σ_t) is a point in either of the stress régimes R_1 and R_2 while plastic cycling occurs in the stress régime P. Shakedown occurs after the first half-cycle in the stress régimes S_1 and S_2 and purely elastic behaviour is experienced in the stress régime E.

To illustrate the method of calculating the strains it will be sufficient to consider only the ratchetting régime R_1 and the plastic-cycling régime P. The distributions of stress and plastic strain incurred by each cycle for the stress régime R_1 are shown in Fig. 4. Since $\sigma_p + \sigma_t > \sigma_Y$, it follows from equation (8) that the can material yields in tension in a region adjacent to the outer surface during the first half-cycle. If the elastic–plastic interface occurs at $x = a$, then σ and $E\eta$ have the forms shown in Figs 4*a* and 4*b*, where the oblique lines have slope $2\sigma_t/d$. It follows from the mean stress condition that a is given by

$$a = -\tfrac{1}{2}d\{1 - 2\sqrt{(\sigma_Y - \sigma_p)/\sigma_t}\} \quad . \quad . \quad (16)$$

and since $\sigma_p + \frac{1}{4}\sigma_t > \sigma_Y$ in the stress régime R_1, $a < 0$ as shown. Consequently, on shutdown of the reactor the can material will yield in a region adjacent to the inner surface, resulting in the stress distribution shown in Fig. 4*c* where the oblique line has slope $-2\sigma_t/d$. Since σ and $E\eta$ must have equal and opposite slopes at each point, the plastic strain incurred by shutdown is that shown in Fig. 4*d*. When the temperature gradient is reimposed, the can material yields again in the region $x > a$, giving once more the stress of Fig. 4*a* and the additional plastic strain

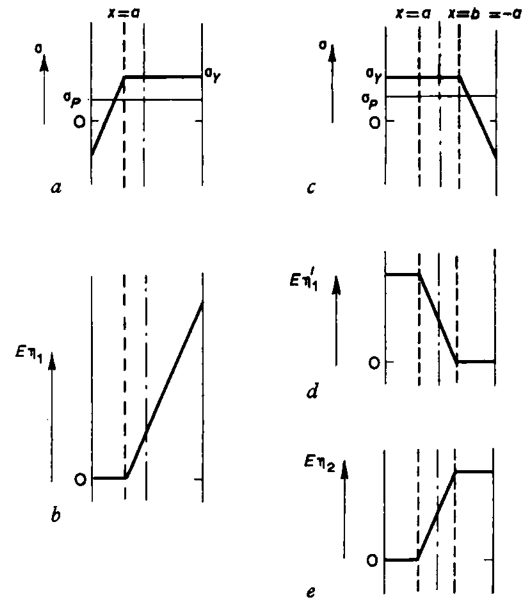

a Stress incurred by first half of each cycle.
b Plastic strain incurred by first half-cycle.
c Stress incurred by second half of each cycle.
d Plastic strain incurred by second half of each cycle.
e Plastic strain incurred by first half of each cycle after the first.

Fig. 4. Distributions of stress and plastic strain incurred by each half-cycle for the stress régime R_1 *of Fig. 3*

of Fig. 4*e*. Thereafter a steady-state cycle is established in which the plastic strains incurred by each start-up and shutdown are those shown in Figs 4*e* and 4*d*. The increment of strain per cycle is the sum of these two strains, which is therefore given by

$$\delta = (2\sigma_t/E)\{1 - 2\sqrt{(\sigma_Y - \sigma_p)/\sigma_t}\} \quad . \quad (17)$$

The stress σ_e having been introduced by the relation

$$\sigma_e = \sigma_p + \tfrac{1}{4}\sigma_t - \sigma_Y \quad . \quad . \quad . \quad (18)$$

equation (17) may be written in the form

$$E\delta/2\sigma_t = 1 - (1 - 4\sigma_e/\sigma_t)^{1/2} \quad . \quad . \quad (19)$$

and the graph of $E\delta/2\sigma_t$ against σ_e/σ_t is the parabola shown in Fig. 5. If $\sigma_e \ll \frac{1}{4}\sigma_t$, equation (19) reduces to

$$\delta = 4\sigma_e/E \quad . \quad . \quad . \quad . \quad (20)$$

approximately, which is represented by the straight line in Fig. 5. The quantity σ_e may be interpreted as an excess stress since it measures the amount by which $\sigma_p + \frac{1}{4}\sigma_t$ exceeds σ_Y or the extent to which the ratchetting régime R_1 is penetrated.

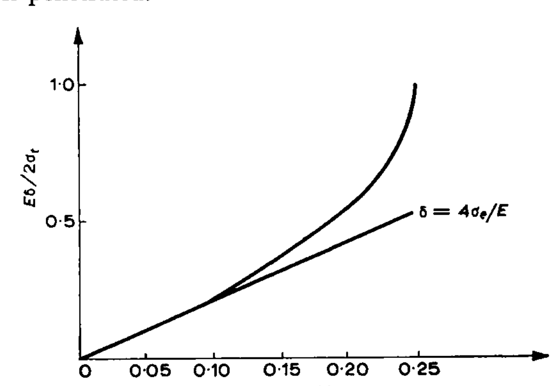

Fig. 5. Ratchet strain per cycle for the stress régime R_1 *of Fig. 3*

It is easily verified from the stress of Fig. 4*a* that the can material also yields in compression at the inner surface during the first half-cycle if $\sigma_t(\sigma_y - \sigma_p) > \sigma_y^2$. The distributions of stress and plastic strain are then as shown in Figs 6*a* and 6*b*, where the oblique lines have slope $2\sigma_t/d$ and the elastic–plastic interfaces are given by

$$\left.\begin{aligned} a &= \tfrac{1}{2}d(\sigma_y/\sigma_t - \sigma_p/\sigma_y) \\ b &= -\tfrac{1}{2}d(\sigma_y/\sigma_t + \sigma_p/\sigma_y) \end{aligned}\right\} \quad . \quad . \quad (21)$$

If (σ_p, σ_t) is a point in the stress régime P, then $\sigma_p\sigma_t < \sigma_y^2$ (which corresponds to $a > 0$) and $\sigma_t > 2\sigma_y$. The can material therefore yields at both surfaces during shutdown, giving the stress and additional plastic strain of Figs 6*c* and 6*d* where the elastic–plastic interfaces $x = c$ and $x = -c$ are given by

$$c = (\sigma_y/\sigma_t)d \quad . \quad . \quad . \quad . \quad (22)$$

On re-application of the temperature gradient we obtain once more the stress of Fig. 6*a* and the additional plastic strain of Fig. 6*e*. Since the sum of the plastic strains shown in Figs 6*d* and 6*e* is zero the can ceases to grow after the first half-cycle but cyclic plastic strains occur in the region $|x| > c$, the plastic strain range being given by

$$2(|x| - c)\sigma_t/Ed$$

This has its maximum value

$$\epsilon_c = (\sigma_t - 2\sigma_y)/E \quad . \quad . \quad . \quad (23)$$

at both the inner and outer surfaces of the can wall and hence fatigue failure will first occur at these points. The stress–strain path at $x = \frac{1}{2}d$ is shown in Fig. 7 where σ is plotted against $\epsilon - \alpha T$. The state of stress and strain follows the path ABCDE during the first cycle, then

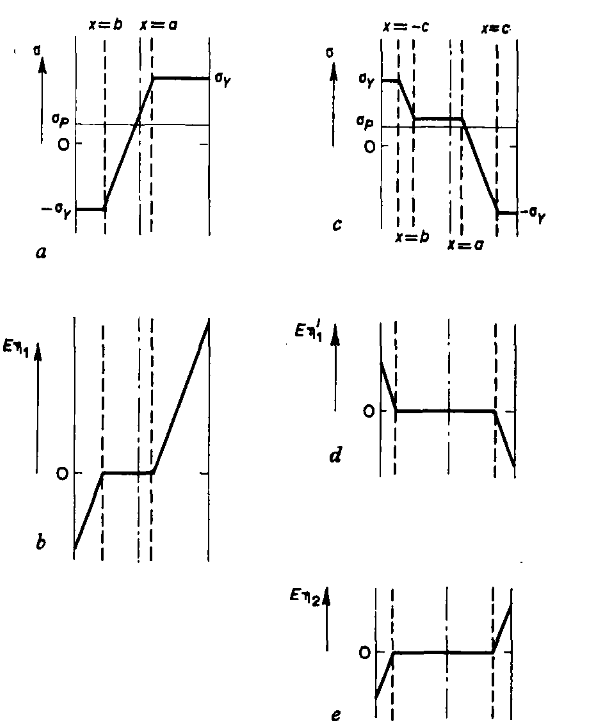

a Stress incurred by first half of each cycle.
b Plastic strain incurred by first half-cycle.
c Stress incurred by second half of each cycle.
d Plastic strain incurred by second half of each cycle.
e Plastic strain incurred by first half of each cycle after the first.

Fig. 6. Distributions of stress and plastic strain incurred by each half-cycle for the stress régime P *of Fig. 3*

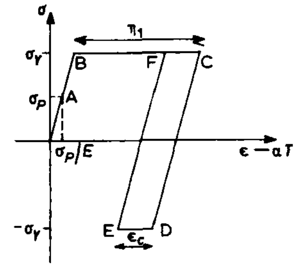

Fig. 7. Stress–strain path at $x = \frac{1}{2}d$ corresponding to the stress régime P *of Fig. 3*

repeats the hysteresis loop EFCDE every subsequent cycle, reaching the point C at the end of each start-up and the point E at the end of each shutdown. Thus a net amount of irreversible plastic work, equal to the area of the hysteresis loop, is done per unit volume per cycle at $x = \frac{1}{2}d$ which must ultimately weaken the can. This fatigue problem has been extensively studied by many experimental investigators and in particular by Coffin (1) who derived the empirical relation

$$N = \epsilon_f^2/4\epsilon_c^2$$

where N is the number of cycles to failure and ϵ_f is the tensile ductility of the material. Hence the number of cycles to failure is given by

$$N = \epsilon_f^2E^2/4(\sigma_t - 2\sigma_y)^2 \quad . \quad . \quad (24)$$

If, however, the can experiences n cycles, failure will not occur by fatigue cracking provided

$$\sigma_t - 2\sigma_y < E\epsilon_f/2(n)^{1/2}$$

In the stress régime R_2, ratchetting occurs with combined tensile and compressive yielding and the increment of strain per cycle is given by

$$\delta = (2\sigma_t/E)(\sigma_p/\sigma_y - \sigma_y/\sigma_t) \quad . \quad . \quad (25)$$

In addition, during each cycle the material in $|x| > b$ undergoes a hysteresis loop of width

$$2(|x| + b)\sigma_t/Ed$$

which has its maximum value

$$\epsilon_c = (\sigma_t - \sigma_y - \sigma_p\sigma_t/\sigma_y)/E \quad . \quad . \quad (26)$$

at $|x| = \frac{1}{2}d$. The stress strain path at $x = \frac{1}{2}d$ is illustrated in Fig. 8, where it is shown that the state of stress and strain follows the path $ABC_1D_1E_1F_1C_2D_2E_2F_2C_3$, etc. and reaches the point C_n at the end of the nth start-up and the point E_n at the end of the nth shutdown.

It is of interest to note that the above results also hold for a slab subjected to a uniaxial load σ_p and a variable bending moment in the same direction which cycles the

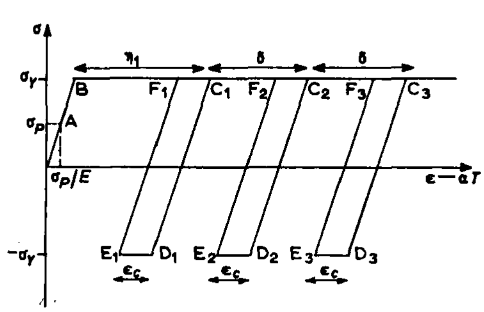

Fig. 8. Stress–strain path at $x = \frac{1}{2}d$ corresponding to the stress régime R_2 *of Fig. 3*

curvature between a specific value ρ and zero, where σ_t and ρ are related by

$$\sigma_t = \tfrac{1}{2}\rho E d$$

However, $2x\sigma_t/Ed$ must be subtracted from the total strain ϵ during the first half of each cycle to obtain the corresponding total strain in bending. Edmunds and Beer (6) have examined problems in the bending of a plate where the bending occurs in one direction only and the plate is loaded biaxially.

EFFECT OF MEAN TEMPERATURE ON YIELD STRENGTH

On shutdown of the reactor, the mean temperature of the can is reduced so that the value of the yield stress is, in general, greater than its value on shutdown. To estimate the effect of this it is assumed that the yield stress σ'_y on shutdown differs from its value on start-up and that the temperature variation across the can wall does not cause a significant variation of σ_y so that this may be supposed constant. Work-hardening is ignored.

Methods similar to those used in the previous section reveal the various stress régimes to be as shown in Fig. 9, the notation being similar to that used in Fig. 3. For the ratchetting régimes R_1 and R_2 the respective increments of strain per cycle are

$$\delta = (2\sigma_t/E)\{1-\sqrt{(\sigma_y-\sigma_p)/\sigma_t}-\sqrt{(\sigma'_y-\sigma_p)/\sigma_t}\} \quad (27)$$

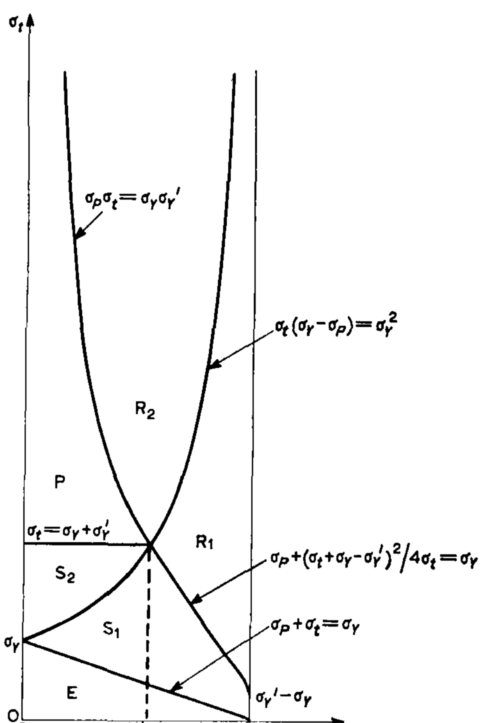

Stress régime	Can behaviour
R_1 and R_2	Ratchetting
S_1 and S_2	Shakedown after first half-cycle
P	Plastic cycling
E	Elastic

Fig. 9. Stress régimes for non-work-hardening material whose yield stress varies between σ_y at start-up and σ'_y at shutdown owing to changes in mean temperature

and

$$\delta = (\sigma_y+\sigma'_y)(\sigma_p\sigma_t-\sigma_y\sigma'_y)/E\sigma_y\sigma'_y \quad . \quad (28)$$

For the plastic-cycling régime P, the maximum value of the plastic-strain range, which occurs at $|x| = \tfrac{1}{2}d$, is given by

$$\epsilon_c = [\sigma_t-(\sigma_y+\sigma'_y)]/E \quad . \quad . \quad . \quad (29)$$

Hence, according to Coffin's law, the number of cycles to failure is given by

$$N = E^2\epsilon_f^2/4[\sigma_t-(\sigma_y+\sigma'_y)]^2$$

and fatigue failure may be avoided by imposing the condition

$$\sigma_t-(\sigma_y+\sigma'_y) < E\epsilon_f/2(n)^{1/2}$$

where n is the number of cycles experienced by the can.

Finally, in the stress régimes S_1 and S_2 shakedown occurs after the first half-cycle and the can's behaviour is purely elastic in the stress régime E.

EFFECT OF WORK-HARDENING

The analysis so far assumes that the can material is non-work-hardening. Consequently, the growth of the can under ratchetting and the plastic-strain range during fatigue are the same for each cycle after the first. In practice, however, the material work-hardens, that is the stress in the plastic range increases with increasing plastic strain. Effectively this means that the yield stress increases with each cycle so that the magnitude of the plastic strains incurred by each cycle decreases and must ultimately be reduced to zero. To estimate the effect of work-hardening we will assume a linear rate of hardening, that is the plastic part of the uniaxial stress–strain curve is assumed to have constant slope. The initial yield stress σ_y marks the transition from the elastic to the plastic part of the curve and is assumed to be independent of the mean temperature. For the uniaxial model a linear rate of hardening implies that plastic yielding occurs during any half-cycle only if the stress σ calculated for purely elastic changes of state during the half-cycle is such that (5)

$$|\sigma| > \sigma_y + k\textstyle\sum' |\eta|$$

where $\sum' |\eta|$ is the sum of the moduli of the plastic strains incurred by the preceding half-cycles. In regions where the material yields, plastic strains are introduced to relieve the stress to a value which satisfies the equation (5)

$$|\sigma| = \sigma_y + k\textstyle\sum |\eta|$$

where $\sum |\eta|$ is defined similarly to $\sum' |\eta|$ except that it also includes the plastic strain incurred by the current half-cycle. The proportionality constant k is given by

$$k = EE_1/(E-E_1) \quad . \quad . \quad . \quad (30)$$

where E_1 is the slope of the uniaxial stress–strain curve in the plastic range. Thus if $E_1 \ll E$, as is usually the case, then $k \simeq E_1$.

Owing to the algebraic complexity introduced by work-hardening it is convenient to make certain simplifying assumptions. When ratchetting is under consideration we will assume that purely tensile plastic flow occurs during each cycle which corresponds to the stress régime R_1 of Fig. 3. This greatly restricts the range of values of σ_p and σ_t for which the calculation is valid. Roughly, if $k \ll E$, the results will be valid provided $\sigma_t - \sigma_p < 3\sigma_y/2$ and $\sigma_p + \tfrac{1}{4}\sigma_t > \sigma_y$ but may be applied pessimistically for all values of σ_p and σ_t. In non-work-hardening material the criterion for the onset of plastic cycling and the plastic-strain range are independent of σ_p. This will still be approximately true even when work-hardening is accounted for. Hence, to estimate the effect of work-hardening in the plastic-cycling régime, it will be sufficient to consider the case when σ_p is zero.

Ratchetting with purely tensile yielding

On the assumption that plastic flow is purely tensile, it is found that ratchetting occurs in material with a linear rate of hardening only if

$$\sigma_p+E\sigma_t/4(E+k) > \sigma_y \quad . \quad . \quad . \quad (31)$$

The distributions of stress and plastic strain are then found to be given by the following formulae.

For the nth start-up

$$\sigma = \begin{cases} \sigma_y+k\lambda_{(n-1)}+2(x-a_n)\sigma_t/d & (-\tfrac{1}{2}d \leqslant x \leqslant a_n) \\ \sigma_y+k\lambda_{(n-1)}+2k(x-a_n)\sigma_t/(E+k)d & (a_n \leqslant x \leqslant \tfrac{1}{2}d) \end{cases}$$

$$\eta = \begin{cases} \lambda_{(n-1)} & (-\tfrac{1}{2}d \leqslant x \leqslant a_n) \\ \lambda_{(n-1)}+2(x-a_n)\sigma_t/(E+k)d & (a_n \leqslant x \leqslant \tfrac{1}{2}d) \end{cases}$$

$$\epsilon = \sigma_y/E+(1+k/E)\lambda_{(n-1)}-2a_n\sigma_t/Ed$$

while for the nth shutdown these are given by

$$\sigma = \begin{cases} \sigma_y+k\lambda_{(n)} & (-\tfrac{1}{2}d \leqslant x \leqslant b_n) \\ \sigma_y+k\lambda_{(n)}-2E(x-b_n)\sigma_t/(E+k)d & (b_n \leqslant x \leqslant \tfrac{1}{2}d) \end{cases}$$

$$\eta = \begin{cases} \lambda_{(n)} & (-\tfrac{1}{2}d \leqslant x \leqslant b_n) \\ \lambda_{(n)}+2(x-b_n)\sigma_t/(E+k)d & (b_n \leqslant x \leqslant \tfrac{1}{2}d) \end{cases}$$

$$\epsilon = \sigma_y/E+(1+k/E)\lambda_{(n)}$$

where the can material yields in the region $x > a_n$ during the nth start-up and in the region $x < b_n$ during the nth shutdown and

$$\lambda_{(n)} = \sum_{i=1}^{n} 2(b_i-a_i)\sigma_t/(E+k)d$$

The elastic–plastic boundaries, $x = a_n$ and $x = b_n$, may be calculated from the sequence

$$\left.\begin{aligned} a_n &= -\tfrac{1}{2}d(1+2k/E) \\ &\qquad +d\sqrt{(1+k/E)[k/E+k\lambda_{(n-1)}/\sigma_t+(\sigma_y-\sigma_p)/\sigma_t]} \\ b_n &= \tfrac{1}{2}d(1+2k/E) \\ &\quad -d\sqrt{(1+k/E)[k/E+k\lambda_{(n-1)}/\sigma_t+(\sigma_y-\sigma_p)/\sigma_t]}-2ka_n/Ed \end{aligned}\right\} \quad . \quad . \quad . \quad (32)$$

It may be shown that the condition (31) implies that $a_n < 0$ and $b_n > 0$ for all n and, as a consequence of work-hardening, a_n increases monotonically to zero and b_n decreases monotonically to zero as n increases. Hence, from equation (32), it follows that

$$\lim_{n\to\infty} k\lambda_{(n)} = \sigma_p-\sigma_y+M\sigma_t$$

where

$$M = E/4(E+k)$$

Therefore as n tends to infinity, the stress at start-up tends to

$$\sigma = \begin{cases} \sigma_p+M\sigma_t+2x\sigma_t/d & (-\tfrac{1}{2}d \leqslant x \leqslant 0) \\ \sigma_p+M\sigma_t+2kx\sigma_t/(E+k)d & (0 \leqslant x \leqslant \tfrac{1}{2}d) \end{cases}$$

and the stress at shutdown tends to

$$\sigma = \begin{cases} \sigma_p+M\sigma_t & (-\tfrac{1}{2}d \leqslant x \leqslant 0) \\ \sigma_p+M\sigma_t-2Ex\sigma_t/(E+k)d & (0 \leqslant x \leqslant \tfrac{1}{2}d) \end{cases}$$

Similar asymptotic expressions may be obtained for the strains. In particular, the limiting stress at the can mid-wall is given by

$$\sigma'_L = \sigma_p+E\sigma_t/4(E+k) \quad . \quad . \quad (33)$$

and the total strain in the limit corresponds to the stress σ'_L on the uniaxial stress–strain curve.

Plastic cycling with zero pressure stress

As previously stated, we will assume here that the pressure stress is zero. This simplifies the problem considerably without introducing any great loss of generality, since the essential physical features of the problem are still present. With zero pressure stress we can, of course, solve the more accurate biaxial model of the can. However, for the sake of consistency, we will continue to work in terms of the uniaxial model.

When $\sigma_p = 0$, the distributions of stress and plastic strain are anti-symmetrical with respect to the can mid-wall. Their mean values are therefore zero. Consequently, the total strain ϵ, since it is independent of x, is zero at all stages of the deformation. Under these conditions it is found that plastic cycling occurs if

$$\sigma_t > 2E\sigma_y/(E+k)$$

After the first half-cycle the plastic strain is

$$\eta_1 = \begin{cases} 2(x+a)\sigma_t/(E+k)d & (-\tfrac{1}{2}d \leqslant x \leqslant -a) \\ 0 & (-a \leqslant x \leqslant a) \\ 2(x-a)\sigma_t/(E+k)d & (a \leqslant x \leqslant \tfrac{1}{2}d) \end{cases}$$

where $x = a$ and $x = -a$ are the elastic–plastic boundaries which are determined by

$$a = (\sigma_y/2\sigma_t)d$$

The plastic strains incurred by all subsequent half-cycles are given by

$$\eta_n = \left\{\begin{array}{ll} 2R^{2(n-1)}(x+b)\sigma_t/(E+k)d & (-\tfrac{1}{2}d \leqslant x \leqslant -b) \\ 0 & (-b \leqslant x \leqslant b) \\ 2R^{2(n-1)}(x-b)\sigma_t/(E+k)d & (b \leqslant x \leqslant \tfrac{1}{2}d) \end{array}\right\} \quad . \quad . \quad . \quad (34)$$

for the nth start-up, and

$$\eta'_n = \left\{\begin{array}{ll} -2R^{2n-1}(x+b)\sigma_t/(E+k)d & (-\tfrac{1}{2}d \leqslant x \leqslant -b) \\ 0 & (-b \leqslant x \leqslant b) \\ -2R^{2n-1}(x-b)\sigma_t/(E+k)d & (b \leqslant x \leqslant \tfrac{1}{2}d) \end{array}\right\} \quad . \quad . \quad . \quad (35)$$

for the nth shutdown, where

$$R = (E-k)/(E+k)$$

and $x = b$ and $x = -b$ $(b > a)$ are the elastic–plastic boundaries, given by

$$b = E\sigma_y d/(E-k)\sigma_t$$

It is apparent from equations (34) and (35) that the plastic strains incurred by each half-cycle, apart from the first, constitute the terms of a convergent geometrical progression whose common ratio is $-R$. The solutions for σ and η for the nth cycle are easily obtained by summing the appropriate geometric series and the asymptotic solution then follows by letting n tend to infinity.

The magnitude of the plastic strain produced by each half-cycle is a maximum at $|x| = \tfrac{1}{2}d$. Hence, fatigue cracking will first occur at these points, if at all, and so the plastic strains referred to in the following discussion are assumed to be evaluated at these points. If $k \ll E$, the nth cycle may be regarded as consisting of a cyclic plastic strain ϵ_n which is given approximately by the mean value of the magnitudes of η_n and η'_n, that is

$$\epsilon_n = \tfrac{1}{2}(\eta_n - \eta'_n)_{x=\frac{1}{2}d} \quad . \quad . \quad . \quad (36)$$

The first cycle consists of a monotonic plastic strain together with a cyclic plastic strain. The monotonic strain is usually small compared with the ductility and its contribution to the damage of the material may be neglected, whilst the cyclic strain is given approximately by equation (36), formulae (34) and (35) being used to evaluate η_n and η'_n with $n = 1$. Hence, by a plausible extension of Coffin's law due to Gittus (7), it follows that failure will not occur after N cycles, provided

$$\sum_{n=1}^{N} \epsilon_n^2 < \epsilon_f^2/4$$

On substituting for η_n and η'_n, letting N tend to infinity and retaining only first-order terms in k/E, we find that failure will not occur after any finite number of cycles, provided

$$\sigma_t - 2(1+k/E)\sigma_y < \epsilon_f\sqrt{2kE}(1+k/4E)$$

Usually k/E may be neglected in comparison with unity so that this may be reduced to the simple form

$$\sigma_t - 2\sigma_y < \epsilon_f\sqrt{2kE}$$

EFFECT OF STRESS RELAXATION DUE TO CREEP

The results of the preceding sections apply only if the mean temperature of the can is sufficiently low for creep to be ignored. In practice, while the reactor is at power, the temperature of the can may be so high that creep occurs under the applied stress. On shutdown the mean temperature is reduced so that creep may be ignored throughout the shutdown period.

Creep strain, like plastic strain, is irreversible but, unlike plastic strain which occurs instantaneously with application of the stress, the creep strain is time-dependent. For example, material in a state of creep deforms continuously under a sustained external load. Hence, the pressure stress alone causes the can to grow continuously during the hot part of the temperature cycle. This, however, constitutes a well understood problem which will not concern us here. Here we are primarily interested in those permanent strains which are incurred as a result of cyclic variation of the temperature gradient across the can wall. In addition, creep can effect the relaxation of those stresses which are not necessary to maintain equilibrium with external forces. This is accomplished by a gradual conversion of elastic strain into creep strain. The creep strains so produced increase the residual stresses which occur when the reactor is shut down so that there is a greater tendency for regions of the can material to yield during the second part of the temperature cycle. This, of course, results in further ratchetting and plastic cycling.

Since the extent to which the non-uniform stress relaxes depends on the time the reactor is at power and on the creep law for the material which is, in general, non-linear, a detailed analysis of the effect of creep is difficult to obtain. Even with the simple slab model this can only be achieved numerically and requires the strain path to be calculated step by step as time proceeds during each cycle and for different values of σ_p and σ_t. However, using the uniaxial model, we will attempt to assess the maximum possible effect of creep by making the pessimistic assumption that maximum creep relaxation of the stress occurs while the reactor is at power. This implies that the stress achieves its limiting value prior to shutdown. It is assumed that the can material has uniform creep strength and hence this limiting or steady-state stress is equal to the pressure stress σ_p. Owing to the non-uniform can temperature during the on-power part of the cycle, the creep strength is not uniform as assumed here. The extent to which this affects the results is considered in Appendix 3. In any case, the assumption of uniform creep strength is pessimistic.

With these assumptions, it is in fact found that ratchetting occurs if

$$\sigma_p + \sigma_t > \sigma_y$$

To show this it is sufficient to consider the effect of maximum stress relaxation when (σ_p, σ_t) is a point in the stress régime S_1 of Fig. 3. The can material yields during the first half-cycle in a region adjacent to the outer surface giving the distributions of stress and plastic strain shown in Figs 10*a* and 10*b*. Creep then takes place, causing the stress to relax and the total strain to increase by an amount $\epsilon_c^{(1)}$ which is uniform across the can wall. A permanent creep strain which includes the uniform term $\epsilon_c^{(1)}$ must be introduced to compensate for the change in stress. If the stress relaxes to σ_p, it follows from the stress–strain relation that the total creep plus plastic strain prior to shutdown is

$$\eta = \epsilon_c^{(1)} + (\sigma_y - \sigma_p)/E + 2(x-a)\sigma_t/Ed \quad . \quad (37)$$

where a is given by equation (16). Apart from the uniform term $\epsilon_c^{(1)}$, the creep strain produced by relaxation of the stress is shown in Fig. 10*c*.

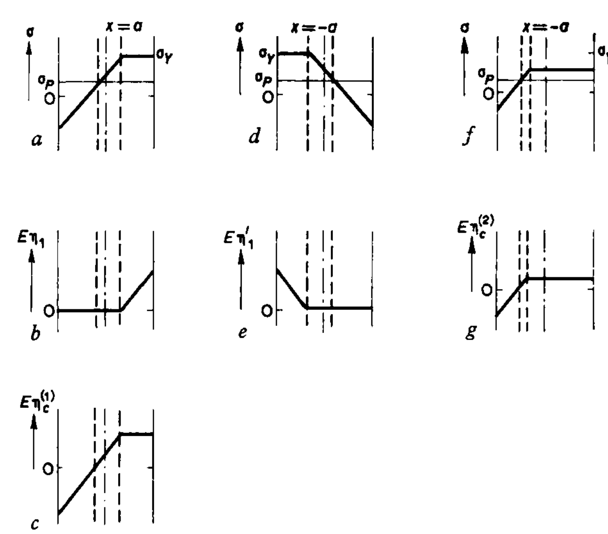

a Stress incurred by first start-up.
b Plastic strain incurred by first start-up.
c Creep strain due to stress relaxation during first cycle.
d Stress incurred by each shutdown.
e Plastic strain incurred by each shutdown.
f Stress incurred by each start-up after the first.
g Creep strain due to stress relaxation during each cycle after the first.

Fig. 10. Distribution of stress, plastic strain, and creep strain incurred by each cycle in the stress régime S_1 *of Fig. 3 when creep causes the stress to relax to* σ_p *before each shutdown*

The stress is now equal to σ_p and, since $\sigma_p+\sigma_t > \sigma_y$, removal of the temperature gradient causes the can material to yield in tension in a region adjacent to the inner surface, giving the distributions of stress and additional plastic strain shown in Figs 10*d* and 10*e*. Since the mean temperature is reduced, creep does not take place while the reactor is shut-down. Hence, the total strain throughout the shutdown is given by

$$\epsilon = \epsilon_c^{(1)}+(2\sigma_y-\sigma_p)/E-4a\sigma_t/Ed \quad . \quad (38)$$

The can material does not yield on start-up of the reactor since $\sigma_p+\frac{1}{2}\sigma_t < \sigma_y$. The stress then has the form shown in Fig. 10*f* and, since no further plastic strain is incurred by start-up, the total strain ϵ is given by equation (38). Creep now causes the total strain to increase by the uniform amount $\epsilon_c^{(2)}$ as the stress relaxes to σ_p so that equation (38) together with the stress–strain relation yields

$$\eta = \epsilon_c^{(1)}+\epsilon_c^{(2)}+2(\sigma_y-\sigma_p)/E+2(x-2a)\sigma_t/Ed \quad (39)$$

for the total creep plus plastic strain prior to the second shutdown. Thus, apart from $\epsilon_c^{(2)}$, the creep strain produced by relaxation of the stress is shown in Fig. 10*g*.

Since the stress is again uniform prior to shutdown, removal of the temperature gradient will again give the distributions of stress and additional plastic strain of Figs 10*d* and 10*e*. On re-application of the temperature gradient we obtain once more the stress shown in Fig. 10*f* which subsequently relaxes to give the additional creep strain of Fig. 10*g*, together with the uniform increase in strain $\epsilon_c^{(3)}$, and so on for each cycle, a steady-state cycle being established. Thus, apart from the uniform increase in strain produced while the reactor is at power, there is an increment of strain per cycle equal to the sum of the strains shown in Figs 10*e* and 10*g*. Hence ratchetting occurs if (σ_p, σ_t) is a point in the stress régime S_1 of Fig. 3 and, by comparison of equations (37) and (39), it follows that the ratchet strain per cycle is given by

$$\delta = (\sigma_y-\sigma_p)/E+(\sigma_t/E)\{1-2\sqrt{(\sigma_y-\sigma_p)/\sigma_t}\}$$

Similarly, it may be shown that ratchetting occurs everywhere in the stress régime $\sigma_p+\sigma_t > \sigma_y$. The ratchet strain per cycle depends on the various stress régimes shown in Fig. 3 as follows:

Stress régime	Ratchet strain per cycle
S_1	$\delta = (\sigma_y-\sigma_p)/E+(\sigma_t/E)\{1-2\sqrt{(\sigma_y-\sigma_p)/\sigma_t}\}$
R_1	$\delta = (\sigma_y-\sigma_p)/E+(2\sigma_t/E)\{1-2\sqrt{(\sigma_y-\sigma_p)/\sigma_t}\}$
S_2, P	$\delta = (\sigma_y-\sigma_p)/E+(\sigma_t/E)\{\sigma_p/\sigma_y-\sigma_y/\sigma_t\}$
R_2	$\delta = (\sigma_y-\sigma_p)/E+(2\sigma_t/E)\{\sigma_p/\sigma_y-\sigma_y/\sigma_t\}$

. . . (40)

Thus ratchetting now occurs in those stress régimes where shakedown and plastic cycling occurred in the absence of creep, and in the stress régimes where ratchetting previously occurred the ratchet strain per cycle is increased by the amount $(\sigma_y-\sigma_p)/E$. It should be remembered that the total increment of strain per cycle is given by

$$\delta^{(n)} = \delta+\epsilon_c^{(n)}$$

where $\epsilon_c^{(n)}$, which depends on the creep law and the time the reactor is at power, is the uniform increase in strain produced while the reactor is at power during the *n*th cycle. Owing to the interaction of the thermal stress with the pressure stress, $\epsilon_c^{(n)}$ is, in general, greater than the creep strain which would result from the pressure stress alone. This enhanced creep strain occurs only when the creep law for the material is non-linear. A method of calculating the enhanced creep strain as well as the ratchet strain per cycle, when only partial stress relaxation occurs while the reactor is at power, is to be published in a future paper. Finally, if $\sigma_p+\sigma_t < \sigma_y$, the stress relaxes to σ_p during the first half-cycle giving a permanent creep strain

$$\eta = \epsilon_c^{(1)}+2x\sigma_t/Ed$$

and thereafter no further permanent strain is produced other than that produced by creep under the pressure stress alone.

DISCUSSION

Using the simple model developed in the first section we have been able to predict the approximate stress–strain behaviour in the hoop direction of a fuel can consisting of a long thin tube with closed ends when subjected to intermittent high heat fluxes in the presence of a sustained internal pressure. Various assumptions are made about the can material and the mechanisms of deformation. These, however, are stated as they arise in the following discussion of the results.

For a can constructed of non-work-hardening material with a yield stress independent of temperature, ratchetting occurs if (σ_p, σ_t) is a point in the stress régimes R_1 and R_2 of Fig. 3 and the corresponding increments of strain per cycle are given by equations (17) and (25). Examples of the contours of constant ratchet strain per cycle are shown in Fig. 11. If (σ_p, σ_t) lies in the stress régime P of Fig. 3,

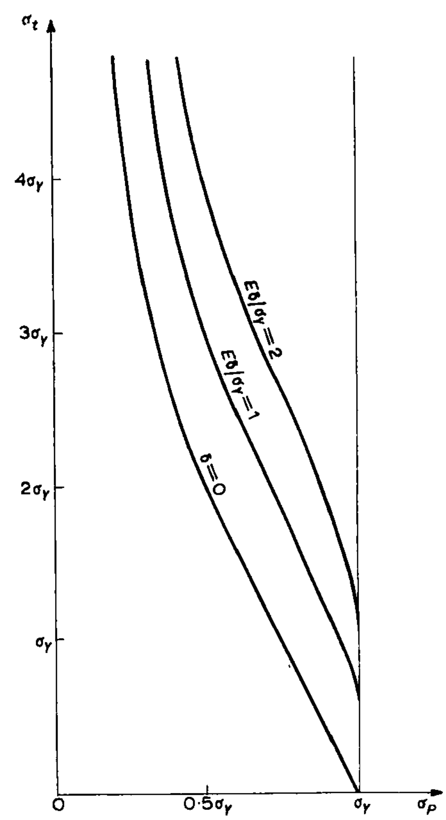

Fig. 11. Lines of constant ratchet strain per cycle for non-work-hardening material whose yield stress remains unchanged by changes in mean temperature

plastic cycling occurs and the maximum value of the plastic-strain range is given by equation (23). Ratchetting may therefore be avoided by employing the following safety criteria:

$$\left.\begin{aligned} \sigma_p+\tfrac{1}{4}\sigma_t < \sigma_y \quad &\text{when} \quad \sigma_p > \tfrac{1}{2}\sigma_y \\ \sigma_p\sigma_t < \sigma_y^2 \quad &\text{when} \quad \sigma_p < \tfrac{1}{2}\sigma_y \end{aligned}\right\} \quad . \quad (41)$$

and plastic cyling may be avoided by imposing the condition

$$\sigma_t < 2\sigma_y \quad \text{when} \quad \sigma_p < \tfrac{1}{2}\sigma_y \quad . \quad (42)$$

These are the well known criteria which were first obtained by Miller (**2**).

According to Coffin's law, the number of cycles to failure under plastic cycling is given by equation (24). If we assume $\sigma_t-2\sigma_y = 5000$ lb/in^2, $E = 2\times10^7$ lb/in^2, and the ductility after irradiation is only 1 per cent, the number of cycles to failure $N = 400$. Similarly, $N = 100$ if $\sigma_t-2\sigma_y = 10\,000$ lb/in^2. Now, typically, with $\sigma_y = 15\,000$ lb/in^2, the third criterion implies that σ_t should not exceed 30 000 lb/in^2. The present calculations suggest that fatigue failure is unlikely if σ_t exceeds this value by 20 per cent or perhaps even 40 per cent, provided the can retains some ductility after irradiation, and provided that the increase of σ_t does not cause ratchetting. There does not appear to be the same margin of safety before failure occurs because of ratchetting. For example, if $\sigma_p = \frac{1}{2}\sigma_y$, ratchetting occurs if $\sigma_t > 2\sigma_y$, and from equation (25) the ratchet strain is $(\sigma_t-2\sigma_y)/E$ per cycle, or $2{\cdot}5\times10^{-4}$ per cycle if $\sigma_t-2\sigma_y = 5000$ lb/in^2. Apart from considerations of ductility the strain may be limited to about 1 per cent, say, by the effect on coolant flow rate, corresponding to only 40 cycles. It would thus appear that the ratchetting criteria constitute a real limitation on permissible can stresses while the plastic-cycling criterion is unduly restrictive and may be replaced by a criterion based on Coffin's law, viz.

$$\sigma_t-2\sigma_y < E\epsilon_f/2(n)^{1/2} \quad \text{when} \quad \sigma_p\sigma_t < \sigma_y^2 \quad (43)$$

where n is the number of cycles to be experienced by the can.

Reduction of the can mean temperature during shutdown may be sufficient to cause a significant increase in the yield stress from σ_y to σ'_y, in which case the ratchetting and plastic-cycling stress régimes are as shown in Fig. 9. Hence, the appropriate criteria to avoid ratchetting are

$$\left.\begin{aligned} \sigma_p+(\sigma_t+\sigma_y-\sigma'_y)^2/4\sigma_t < \sigma_y \quad &\text{when } \sigma_p > \sigma_y\sigma'_y/(\sigma_y+\sigma'_y) \\ \sigma_p\sigma_t < \sigma_y\sigma'_y \quad &\text{when } \sigma_p < \sigma_y\sigma'_y/(\sigma_y+\sigma'_y) \end{aligned}\right\} \quad . \quad . \quad . \quad (44)$$

and to avoid plastic cycling

$$\sigma_t < \sigma_y+\sigma'_y \quad \text{when} \quad \sigma_p < \sigma_y\sigma'_y/(\sigma_y+\sigma'_y) \quad (45)$$

The increments of strain per cycle corresponding to the ratchetting régimes R_1 and R_2 are given by equations (27) and (28), respectively, and for the plastic-cycling régime P the maximum value of the plastic-strain range is given by equation (29). The general conclusions, however, remain unchanged, viz. that the ratchetting criteria are real limiting criteria whereas the criterion to avoid plastic cycling is too restrictive and may be replaced by the alternative criterion,

$$\sigma_t-(\sigma_y+\sigma'_y) < E\epsilon_f/2(n)^{1/2} \quad \text{when} \quad \sigma_p\sigma_t < \sigma_y\sigma'_y \quad (46)$$

based on Coffin's law.

When work-hardening is accounted for, the Miller criterion to avoid ratchetting becomes $\sigma_p+E\sigma_t/4(E+k) < \sigma_y$, which may be written $\sigma_p+\frac{1}{4}(1-k/E)\sigma_t < \sigma_y$ to the first order in k/E, where k is defined by equation (30). For a typical 316-type stainless steel at 500°C, $k = 5{\cdot}7\times10^5$ lb/in^2 and $E = 2{\cdot}7\times10^7$ lb/in^2. Since $k \ll E$, the ratchetting criterion is not greatly altered by work-hardening. However, it is found that work-hardening causes the increment of strain per cycle to decrease asymptotically to zero after an infinite number of cycles and in the limit the stress at the can mid-wall is $\sigma_p+E\sigma_t/4(E+k)$ or $\sigma_p+\frac{1}{4}(1-k/E)\sigma_t$ to the first order in k/E and the total strain in the limit corresponds to this limiting stress on the uniaxial stress–strain curve. Thus, if σ_T denotes the rupture tensile stress, rupture will not occur provided $\sigma_p+\frac{1}{4}(1-k/E)\sigma_t < \sigma_T$. Alternatively, if the permissible growth of the can is limited to, say, 1 per cent by its effect on coolant flow rate, and σ_K is the tensile stress corresponding to 1 per cent strain, the criterion $\sigma_p+\frac{1}{4}(1-k/E)\sigma_t < \sigma_K$ would apply. Tensile stress–strain measurements on a 316-type steel at 500°C give values of $\sigma_y = 21\,000$ lb/in^2 and $\sigma_K = 26\,000$ lb/in^2. There is, therefore, a considerable margin of safety introduced by work-hardening even for relatively small values of k.

To estimate the effect of work-hardening in the region of plastic cycling, it is sufficient, without any great loss of generality, to consider the case when $\sigma_p = 0$. It is then found that plastic cycling occurs when $\sigma_t > 2E\sigma_y/(E-k)$ or $\sigma_t > 2(1+k/E)\sigma_y$ to the first order in k/E and the plastic-strain range decreases by the constant factor $[(E-k)/(E+k)]^2$ during successive cycles. For a 316-type steel this factor has the value 0·92 and the plastic-strain range is therefore halved after every nine cycles. From a plausible extension of Coffin's law, it follows that the can will not fail by fatigue cracking if

$$\sigma_t-2\sigma_y < \epsilon_f\sqrt{2kE} \simeq 5\times10^6\epsilon_f \text{ lb/in}^2$$

If, for example, $\epsilon_f = 1$ per cent after irradiation, σ_t would have to exceed $2\sigma_y$ by more than 100 per cent for failure to occur at all and then only after a large number of cycles. It would therefore appear that work-hardening precludes the possibility of low-cycle fatigue due to plastic cycling. The calculations, however, assume that the Bauschinger effect (**8**), which would tend to oppose the favourable effect of work-hardening, is not operative.

Since stress relaxation due to creep while the reactor is at power causes the ratchetting and plastic-cycling régimes to be extended, the foregoing results are optimistic when creep is important. An attempt has been made to include the worst possible effect of creep by making the pessimistic assumption that the stress is relaxed by creep to its limiting value while the reactor is at power. Detailed calculations support this assumption for a 316-type steel at 650°C. Assuming the material has a uniform creep strength, we find that ratchetting occurs whenever the thermal stress is sufficient to cause yielding at start-up and hence in this case the criterion to avoid ratchetting is

$$\sigma_p+\sigma_t < \sigma_y \quad . \quad . \quad . \quad . \quad (47)$$

The ratchet strain per cycle depends on the various stress conditions shown in Fig. 3 and is given by equations (40). Contours of constant ratchet strains per cycle are shown in Fig. 12.

Owing to the variation of temperature across the can

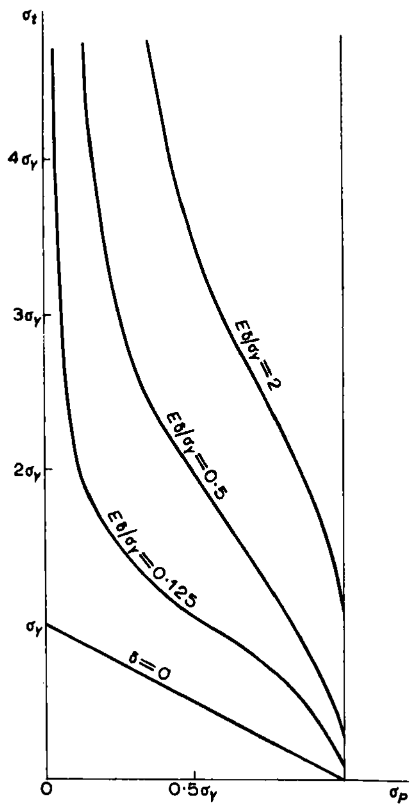

Fig. 12. Lines of constant ratchet strain per cycle when creep causes the stress to relax completely to the pressure stress while the reactor is at power

wall, the creep strength is not in fact uniform. In Appendix 3, where this effect is accounted for, it is shown that the criterion to avoid ratchetting becomes

$$\lambda_1\sigma_p+\sigma_t < \sigma_y \quad . \quad . \quad . \quad . \quad (48)$$

where λ_1 is defined by equation (56) and always has the value 1 when $\sigma_t = 0$. In general λ_1 is a function of σ_t and, for a particular example, is found to decrease steadily from 1 at $\sigma_t = 0$ to about 0·7 at $\sigma_t = \sigma_y$. The corresponding stress régime which causes ratchetting is shown in Fig. 13. As can be seen from the figure or the range of values of λ_1, there is virtually no difference between the ratchetting criteria (47) and (48), although the latter is slightly less restrictive. The calculations of Appendix 3 show that the

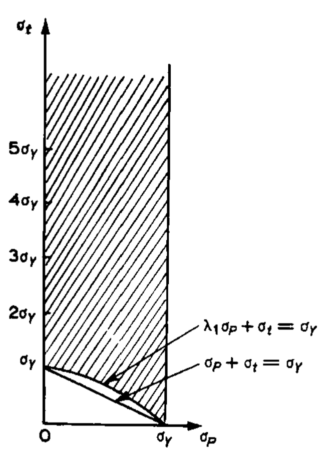

Fig. 13. Ratchetting régime (shaded region) when creep causes the stress to relax to its limiting value while the reactor is at power

non-uniform creep strength has the effect of reducing the ratchet strain per cycle. For example, when $\sigma_p = \frac{1}{2}\sigma_y$, $\sigma_t = \sigma_y$, and typical values are used for material constants, the ratchet strain per cycle, with allowance made for non-uniform creep strength, is $0{\cdot}3\times10^{-4}$ while for uniform creep strength this is $0{\cdot}5\times10^{-4}$. As expected, therefore, the assumption of uniform creep strength is pessimistic.

Some mention should now be made of the effects of irradiation on material properties and possible can behaviour. The effects of irradiation on various cladding materials irradiated to a maximum dose of 5×10^{22} n cm^{-2} in the Dounreay Fast Reactor are reported in (**9**). In particular, for a 316-type stainless steel it is found that irradiation causes an increase in the yield stress and a reduction in the ductility at test temperatures up to about 650°C. For example, at 600°C the solution-treated material shows an increase in yield stress from 18×10^3 lb/in^2 to 37×10^3 lb/in^2 and a reduction in ductility from 50 to 30 per cent after irradiation to a total dose of $3{\cdot}6\times10^{22}$ n cm^{-2}. The change in mechanical properties at low temperature is a function of the total dose and saturation of the hardening effect was evident at 2 and 3×10^{22} n cm^{-2}. At test temperatures above 650°C irradiation has little effect on the yield stress but causes a progressive decrease in ductility which becomes more marked as the test temperature increases. These results imply that the criteria to avoid ratchetting and plastic cycling are likely to be less restrictive when account is taken of irradiation hardening at temperatures below 650°C while at temperatures above 650°C they are not likely to be affected by irradiation. Owing to the reduction in ductility as a result of irradiation, especially at the higher temperatures, care should be taken when the fatigue criterion based on Coffin's law is employed.

Finally, it is necessary to discuss the likely accuracy of the results obtained by the uniaxial stress model when applied to a thin can. The main assumption made in the construction of the mathematical model is that the stress in the axial direction is zero. However, to some extent this is compensated for by introducing the correction factor $(1-\nu)^{-1}$ in the temperature gradient. This has the effect of making the thermal stress in the model equal to the thermal stress in the can. It is shown in Appendix 1 that the effect of a stress equal to the hoop stress acting in the axial direction is to reduce the hoop strains by the factor $(1-\nu)$ while the ratchetting and plastic-cycling criteria remain unchanged. In the thin can the hoop and axial thermal stresses are equal but the mean value of the axial stress is only half of the mean hoop stress. This suggests that the hoop strains in the can lie between 1 and $(1-\nu) \simeq \frac{2}{3}$ times those predicted by the uniaxial model and that the ratchetting and plastic-cycling criteria hold approximately for a thin can. In particular, when $\sigma_p = 0$, the strain correction factor is exactly $(1-\nu)$ and the plastic-cycling criterion is exact. By means of the Tresca yield criterion, it is shown in Appendix 2 that the criterion for the onset of ratchetting with purely tensile yielding is exactly that predicted by the uniaxial model. Furthermore, with the Tresca yield criterion, it may be shown that the ratchetting criterion (47) also holds exactly for the thin can. It would appear, in fact, that the criterion for ratchetting in the thin can when creep causes the stress to relax to the pressure stress while the reactor is at power, is merely the criterion for yielding whether this be the Tresca, or the von Mises, or any more general yield criterion. These purely theoretical considerations indicate that the behaviour of the thin can is represented approximately by the uniaxial stress model. However, although qualitative agreement with experiment may be expected, it should be emphasized that experimental correlation is essential before the numerical results predicted by the model can be used with confidence.

CONCLUSIONS

The following conclusions are drawn from the theory.

The criteria for the onset of ratchetting and plastic cycling predicted by the uniaxial stress model hold approximately for a thin can and are sometimes accurate on the basis of the Tresca yield criterion.

The plastic hoop strains in a thin can lie between 1 and $(1-\nu)$ times those predicted by the uniaxial model.

For non-work-hardening material with a yield stress independent of temperature, ratchetting occurs in the stress régimes R_1 and R_2 and plastic cycling in the stress régime P of Fig. 3.

When the change in mean temperature during shutdown causes a significant increase in the yield stress, the ratchetting régimes R_1 and R_2 and the plastic-cyling régime P are shown in Fig. 9.

The criteria to avoid ratchetting constitute a real limitation on permissible can stresses, whereas the criteria to avoid plastic cycling appear unduly restrictive and may be replaced by criteria based on Coffin's law. However, care should be taken in the application of Coffin's law owing to the reduction in ductility caused by irradiation.

Work-hardening introduces a considerable margin of safety against ratchetting and appears to preclude the possibility of low-cycle fatigue due to plastic cycling. However, it should be emphasized that the Bauschinger effect is neglected in the calculations.

The above conclusions are optimistic when creep is important. Pessimistically, if creep causes the stress to relax to the pressure stress while the reactor is at power, ratchetting occurs if $\sigma_p+\sigma_t > \sigma_y$ and the criterion (47) to avoid ratchetting is then applicable, although this may be relaxed slightly by employing the criterion (48) when account is taken of non-uniform creep strength.

ACKNOWLEDGEMENTS

The author wishes to record his thanks to Mr F. D. Boardman and Mr E. P. Hicks of the Dounreay Experimental Reactor Establishment for many helpful suggestions and discussions.

APPENDIX 1

THIN SPHERICAL SHELL SUBJECTED TO CYCLIC THERMAL STRESSES IN THE PRESENCE OF AN INTERNAL PRESSURE

As a help in assessing the validity of the results predicted by the uniaxial model when applied to a thin can, it is useful to consider the similar problem of thermal cycling in the presence of an internal pressure for a thin spherical shell of radius R and wall thickness d.

The principal components of stress and strain are in the radial, polar, and azimuthal directions r, θ, and ϕ. By symmetry, these quantities depend only on the radial co-ordinate and the stresses, total strains, and plastic strains in the hoop directions θ and ϕ are equal. Hence, in both directions, these may be denoted by σ, ϵ, and η respectively and for a thin shell it may be shown that the radial stress may be neglected compared with σ. As in the thin-can theory, the mean value of the hoop stress remains equal to the pressure stress σ_p throughout the deformation, that is

$$\int_{-1/2d}^{1/2d} \sigma \,dx = \sigma_p d$$

where x is the co-ordinate measured radially outwards from the shell mid-wall. However, σ_p is now given by $PR/2d$ and not, as for thin-can theory, by PR/d.

By virtue of the symmetry, plane radial sections of the shell remain plane radial sections and since $d \ll R$

$$\epsilon = \text{constant}$$

although this constant may vary with each cycle.

Since the state of stress at each point in the material is simply a hydrostatic tension (σ, σ, σ) superposed on a uniaxial compressive stress (σ, 0, 0), both the von Mises and Tresca yield criteria reduce to

$$|\sigma| = \sigma_y \quad \text{(in plastic regions)}$$
$$|\sigma| < \sigma_y \quad \text{(in elastic regions)}$$

Finally, the stress–strain relation in the hoop direction is given by

$$\epsilon = (1-\nu)\sigma/E+\alpha T+\eta$$

where the temperature in the thin shell is given by

$$T = -\Delta Tx/d$$

for the first half of each cycle and is zero for the second half of each cycle. Hence, when substitution is made for T, the stress–strain relation becomes

$$E\epsilon/(1-\nu) = \sigma-2x\sigma_t/d+E\eta/(1-\nu)$$

for the first half of each cycle, and

$$E\epsilon/(1-\nu) = \sigma+E\eta/(1-\nu)$$

for the second half of each cycle.

Now the above equations are precisely those used to determine the stresses and strains in the uniaxial model of the can, except that the strains are divided by the constant factor $(1-\nu)$ and σ_p is now equal to $PR/2d$. The distributions of stress and strain may therefore be obtained from those for the uniaxial model by putting $\sigma_p = PR/2d$ and multiplying the strains by $(1-\nu)$.

The spherical shell is effectively a two-dimensional slab subjected to equal stresses σ in the two perpendicular directions in the plane of the slab, where σ has mean value σ_p and is adjusted to prevent bending in both directions both on application and removal of the temperature gradient. Thus the effect of an equal stress acting in the perpendicular direction in the plane of the slab is to reduce the strains by the factor $(1-\nu)$ while the criteria for the onset of ratchetting and plastic cycling remain unchanged. For a thin cylinder the thermal stresses in both directions are equal but the mean value of the axial stress is only half of the mean hoop stress. Hence for the thin cylinder the strains in the hoop direction must be between 1 and $(1-\nu)$ times those predicted by the uniaxial model. In particular, when $\sigma_p = 0$ the cylindrical can is identical to the spherical shell so that the correction factor is exactly $(1-\nu)$. Moreover, the criteria for the onset of ratchetting and plastic cycling in the thin can must be approximately those predicted by the uniaxial model.

APPENDIX 2

BIAXIAL MODEL OF THE THIN CAN

It has been shown that the thin can is adequately described by a two-dimensional slab subject to mean stresses σ_p and $\frac{1}{2}\sigma_p$ in the hoop and axial directions and prevented from bending in these directions both on application and removal of the temperature distribution

$$T = -\Delta Tx/d$$

The biaxial stress–strain relations are

$$\left.\begin{aligned} \epsilon_\theta &= \sigma_\theta/E-\nu\sigma_z/E+\alpha T+\eta_\theta \\ \epsilon_z &= \sigma_z/E-\nu\sigma_\theta/E+\alpha T+\eta_z \end{aligned}\right\} \qquad (49)$$

For purely elastic deformation $\eta_\theta = \eta_z = 0$. Hence, on substituting for T and remembering that ϵ_θ and ϵ_z are independent of x, we find that equations (49) together with the mean stress conditions (1) give

$$\epsilon_\theta = (2-\nu)\sigma_p/2E, \quad \epsilon_z = (1-2\nu)\sigma_p/2E$$
$$\sigma_\theta = \sigma_p+2x\sigma_t/d, \quad \sigma_z = \sigma_p/2+2x\sigma_t/d$$

From the Tresca yield criterion

$$\text{Max. } \{|\sigma_\theta|, |\sigma_z|, |\sigma_\theta - \sigma_z|\} = \sigma_y$$

it follows that the can material first yields in tension in a region adjacent to the outer surface when the hoop stress at $x = \frac{1}{2}d$ exceeds the yield stress, that is when

$$\sigma_p + \sigma_t > \sigma_y$$

and it may be shown that σ_θ, $(\eta_\theta + \nu\eta_z)/(1-\nu^2)$, $(\epsilon_\theta + \nu\epsilon_z)/(1-\nu^2)$ have the same values as σ, η, ϵ for the uniaxial model. This is as far as the solution can be taken without recourse to numerical methods.

The difficulty of obtaining an analytical solution is now apparent. When the material yields in tension in a region adjacent to the outer surface, the stress in the axial direction is not statically determined. It can only be found in conjunction with the strains by integrating the Levy–Mises flow equation

$$(2\sigma_z - \sigma_\theta)\, d\eta_\theta = (2\sigma_\theta - \sigma_z)\, d\eta_z$$

numerically, step by step as the plastic regions develop during each half-cycle. The same is true of the hoop stress when the material also yields in compression in a region adjacent to the inner surface during the first half-cycle. However, a certain amount of useful information can be obtained analytically if it is assumed that only tensile plastic strains occur during each half-cycle. It then follows from the Tresca yield criterion that the can material yields in tension in a region adjacent to the inner surface during shutdown if

$$\sigma_p + \tfrac{1}{4}\sigma_t > \sigma_y \quad . \quad . \quad . \quad . \quad . \quad (50)$$

and the resulting values of σ_θ, $(\eta_\theta + \nu\eta_z)/(1-\nu^2)$, $(\epsilon_\theta + \nu\epsilon_z)/(1-\nu^2)$ are identical to the values of σ, η, and ϵ for the uniaxial model.

Thereafter a steady-state cycle is established in which the increments of strain per cycle, $\delta\epsilon_0$ and $\delta\epsilon_z$, are related by

$$E(\delta\epsilon_\theta + \nu\delta\epsilon_z)/(1-\nu^2) = 2\sigma_t\{1 - 2\sqrt{(\sigma_y - \sigma_p)/\sigma_t}\}$$

and hence ratchetting occurs if condition (50) is satisfied. It should be noted that the above criterion for the onset of ratchetting with purely tensile yielding is precisely that predicted by the uniaxial model. Similarly, it may be shown that the criterion predicted by the uniaxial model for the onset of ratchetting, on the assumption that creep causes complete stress relaxation while the reactor is at power, also holds exactly for the biaxial model.

APPENDIX 3

THE EFFECT OF NON-UNIFORM CREEP STRENGTH

Owing to the variation of temperature across the can wall, the creep strength of the can material is not uniform as assumed in the section on 'Effect of stress relaxation due to creep'. An attempt is made here to estimate the effect this has on the ratchetting criterion (47) and on the ratchet strain per cycle. For this purpose, it is sufficient to consider the stress régime S_1 of Fig. 3.

The analysis is greatly facilitated by first determining a convenient form for the limiting stress distribution after maximum stress relaxation during the hot part of each cycle. Creep is assumed to occur during the first half of each temperature cycle only and in accordance with the equation for secondary creep which has the general form

$$\dot{\eta} = f(T, \sigma) \quad . \quad . \quad . \quad . \quad . \quad (51)$$

where $\dot{\eta}$ is the creep rate. The temperature T in degrees absolute is given by

$$T = T_0 - \Delta T x/d \quad . \quad . \quad . \quad . \quad (52)$$

where T_0, measured in degrees absolute, is the mean temperature of the can while the reactor is at power. In the limit as the time at power becomes very large, $\dot{\eta}$ tends to the total strain rate $\dot{\epsilon}$ which is independent of x. Equations (51) and (52) then give the limiting or steady-state stress σ_L as a function of x, that is

$$\sigma_L = u(x) \quad . \quad . \quad . \quad . \quad . \quad (53)$$

Equation (53) involves $\dot{\epsilon}$ as an unknown parameter which can be eliminated by means of the mean stress condition. This gives $\bar{u} = \sigma_p$ where $\bar{u}$ is the mean value of $u(x)$. The limiting stress may then be written in the form

$$\sigma_L = \lambda(x)\sigma_p \quad . \quad . \quad . \quad . \quad . \quad (54)$$

where

$$\lambda(x) = u(x)/\bar{u} \quad . \quad . \quad . \quad . \quad . \quad (55)$$

In general, creep rate increases with temperature and with stress. But when the stress has achieved its steady value, the creep rate is independent of x, the temperature (52) decreases with x, and therefore σ_L increases with x. Hence, $\lambda(x)$ is a monotonic increasing function of x whose mean value is unity.

The analysis now follows the same lines as in the section on 'Effect of stress relaxation', except that the stress now relaxes to $\lambda(x)\sigma_p$ instead of σ_p. Under these conditions, it is found that ratchetting occurs if

$$\lambda_1\sigma_p + \sigma_t > \sigma_y$$

where

$$\lambda_1 = \lambda(-d/2) \quad . \quad . \quad . \quad . \quad . \quad (56)$$

Provided $[\lambda(b) - \lambda(\frac{1}{2}d)]\sigma_p > 2b\sigma_t/d$, the ratchet strain per cycle is given by

$$\delta = [\sigma_y - \lambda(b)\sigma_p]/E + 2b\sigma_t/Ed \quad . \quad . \quad . \quad (57)$$

in the stress régime S_1 of Fig. 3, where b is determined by the equation

$$\tfrac{1}{2}\lambda(b)(1-2b/d)\sigma_p + \tfrac{1}{4}(1-2b/d)^2\sigma_t = \sigma_y - \sigma_p + (\sigma_p/d)\int_b^{1/2d} \lambda(x)\, dx \quad . \quad . \quad . \quad (58)$$

Similar expressions may be obtained for the ratchet strain per cycle throughout the stress régime $\lambda_1\sigma_p + \sigma_t > \sigma_y$.

If we now assume a secondary creep law of the form

$$\dot{\eta} = A \exp\{-K/T(x)\}\sigma^n$$

where A, K, and n are material constants, then

$$u(x) = (\dot{\epsilon}/A)^{1/n} \exp\{K/nT(x)\}$$

$$\bar{u} = \frac{1}{d}(\dot{\epsilon}/A)^{1/n}\int_{-1/2d}^{1/2d} \exp\{K/nT(x)\}\, dx$$

and $\lambda(x)$ follows from equation (55). With values of $n = 4$ and $K = 47\,000°\text{C}$, typical of a 316-type stainless steel, and taking $T_0 = 650°\text{C}$, $\Delta T = 45°\text{C}$, and $\sigma_t = 2\sigma_p = \sigma_y = 15\,000$ lb/in², we can solve equation (58) to find $b = -0{\cdot}265d$ and hence $\lambda(b) = 0{\cdot}837$. Thus, if $E = 25 \times 10^6$ lb/in², it follows from equation (57) that $\delta = 0{\cdot}3 \times 10^{-4}$, whereas, for a uniform creep strength, the first of equations (40) gives $\delta = 0{\cdot}5 \times 10^{-4}$. The equation which marks the onset of ratchetting

$$\lambda_1\sigma_p + \sigma_t = \sigma_y \quad . \quad . \quad . \quad . \quad . \quad (59)$$

passes through the points ($\sigma_t = \sigma_y$, $\sigma_p = 0$) and ($\sigma_t = 0$, $\sigma_p = \sigma_y$). The parameter $\lambda_1 = 1$ at $\sigma_t = 0$ and for the above example decreases steadily to $\lambda_1 = 0{\cdot}7$ at $\sigma_t = \sigma_y$. The curve corresponding to equation (59) therefore has the general form shown in Fig. 13.

APPENDIX 4

REFERENCES

(1) COFFIN, L. F. 'A study of the effect of cyclic thermal stresses on a ductile metal', *Trans. Am. Soc. mech. Engrs* 1954 **76**, 931.

(2) MILLER, D. R. 'Thermal-stress ratchet mechanism in pressure vessels', *J. bas. Engng, Trans. Am. Soc. mech. Engrs* 1959 **81**, 190.

(3) LOVE, A. E. H. *The mathematical theory of elasticity*, 4th edition, 1934 (Cambridge University Press).

(4) TIMOSHENKO, S. and GOODIER, J. N. *Theory of elasticity*, 2nd edition, 1951 (McGraw-Hill Book Company, Inc., New York and London).

(5) HILL, R. *The mathematical theory of plasticity* 1950 (Clarendon Press, Oxford).

(6) EDMUNDS, H. G. and BEER, F. J. 'Notes on incremental collapse in pressure vessels', *J. mech. Engng Sci.* 1961 **3**, 187.

(7) GITTUS, J. H. 'General law for the fatigue of bodies having statistically distributed deformability', *Nature* 1965 **206**, 4979.

(8) LUBAHN, J. D. and FELGAR, R. P. *Plasticity and creep of metals* (John Wiley and Sons, Inc., New York).

(9) NETTLEY, P. T. *et al.* 'Problems in the selection and utilization of materials in sodium cooled fast reactors', *Proc. London Conf. Fast Breeder Reactors* 1966 (Pergamon Press Ltd, Oxford).